

# Hot-optical-phonon effects on electron relaxation in an AlGaAs/GaAs quantum cascade laser structure

G. Paulavičius<sup>a)</sup> and V. Mitin

*Department of Electrical and Computer Engineering, Wayne State University, Detroit, Michigan 48202*

M. A. Strosio

*U.S. Army Research Office, P.O. Box 12211, Research Triangle Park, North Carolina 27695-7911*

(Received 16 January 1998; accepted for publication 20 June 1998)

The influence of hot-phonon effects on coupled electron-phonon system relaxation dynamics in an AlGaAs/GaAs quantum cascade laser structure at 10 K has been investigated by the ensemble Monte Carlo technique. The GaAs quantum well laser system considered herein supports lasing between two electron subbands separated by 295 meV. After injection into the upper energy level, electrons transit to the lower subband by means of light emission or phonon-assisted scattering processes. Optical-phonon emission dominates among the latter radiationless electron relaxation channels making the carrier lifetime in the upper subband very short. Therefore, large threshold injection currents are required to create the electron population inversion necessary for lasing; this is one of the most significant shortcomings of quantum cascade lasers. The possibility of increasing the effective lifetime of carriers in the upper laser subband as a result of their return there from the lower subband by means of induced hot-optical-phonon reabsorption was proposed in the literature. However, our simulation results demonstrate that under realistic conditions the role of hot phonons is the opposite: substantial electron heating in the subbands and significant induced optical-phonon emission lead to a reduction in the electron population inversion causing an additional increase in the threshold currents. © 1998 American Institute of Physics. [S0021-8979(98)06518-9]

## I. FORMULATION OF THE PROBLEM

Quantum cascade lasers (QCLs)<sup>1</sup> operate by lasing between electronic subbands in the conduction band which are formed in the semiconductor heterostructure as a result of size quantization. The great advantage of these novel unipolar semiconductor lasers stems from the possibility of tailoring them over a wide spectral range using the same heterostructure material. This material system is usually chosen from technologically mature relatively wide-band-gap semiconductors, such as GaAs and InAs, what facilitates the fabrication of QCL structures without shortcomings of difficult-to-process narrow-band-gap material technology.

Tuning the emission wavelength from the submillimeter to the midinfrared spectral range opens new opportunities for numerous practical applications as well as for experiments that help to clarify the physics of QCL performance. For instance, absorption lines of various vapors and gases can be detected and identified using these lasers.<sup>2</sup> The devices that emit light at wavelengths around 10  $\mu\text{m}$  can be used for spectroscopy and communication applications in the 8–12  $\mu\text{m}$  atmospheric window. Optimization of performance of QCLs to enable continuous-wave operation<sup>2,3</sup> might make this laser a sound alternative for the midinfrared signal range applications.

Starting with the pioneering experimental demonstration of QCL,<sup>1</sup> the physics, the design, and the optimization of these light-emitting devices have been studied extensively as

reported in the literature.<sup>2–9</sup> Pulse-mode and continuous-wave-mode operation of the laser structures at wavelengths of  $\lambda \approx 4.6 \mu\text{m}$  and  $\lambda \approx 8.0 \mu\text{m}$  and for temperatures above liquid-nitrogen temperature was reported in Refs. 2 and 3. Utilizing vertical intersubband electronic transitions, lasing of QCLs was demonstrated recently<sup>7</sup> for operation at temperatures up to room temperature. In Refs. 10 and 11 electron-phonon scattering rates and intersubband optical gain spectra were calculated theoretically taking into account details of optical phonon spectrum in QCL structures; a means of maximizing key electronic transition rates have been proposed as well.

It should be mentioned that despite their obvious merits and extremely attractive features for variety of experiments and practical applications, QCLs suffer from a significant shortcoming—high values of the threshold lasing current. The main reason for this is optical phonon emission which dominates among the radiationless carrier relaxation channels in the active quantum-well (QW) regions. Even though electrons injected in the upper excited state may be prohibited from escaping (by special means such as Bragg reflection) into the continuum, these carriers transfer rapidly to lower subbands through intense optical phonon emissions. This process makes the carrier lifetime in the upper laser subband very short, on the order of magnitude  $10^{-12}$ – $10^{-13}$  s. As a result, large threshold injection currents are required to create the necessary electron population inversion in the active region of a QCL and the efficiency of the laser becomes comparably low.

<sup>a)</sup>Current address: Synopsys, Inc., 700 E. Middlefield Rd., Mountain View, CA 94043-4033.

The process of electron cooling generates a significant nonequilibrium (hot) optical-phonon population what may cause substantial changes in the carrier relaxation kinetics in the system. An important issue is that, in general, QCL structures consist of several stages each of those is formed by an active QW region(s), where photons are generated, and an adjacent electron injector(s), where carriers are thermalized, collected, and reinjected into the next stage. It is well known that spatial confinement of such heterointerface-bounded active quantum-well regions may result in optical phonon confinement.<sup>12</sup> This strongly enhances the influence of hot phonons in such a system in a manner analogous to that of semiconductor nanostructures which display much more pronounced nonequilibrium-phonon buildup than bulk semiconductors.<sup>13–30</sup>

In specific cases, these “captured-within-the-active-region” phonons may greatly influence or even impede the performance of various heterostructure-based quantum devices and microstructures;<sup>8,9,31–45</sup> therefore, these effects must be accurately taken into account in designing such small-scale structures. However, it should be noted that in spite of active research on nonequilibrium electrons and phonons in quantum systems, there is still no adequate understanding of behavior of these structures under strongly pronounced nonequilibrium-phonon conditions in the case of significant carrier-phonon coupling.

Obviously, in the presence of significant hot-phonon feedback, electron cooling rates in the active QCL region become significantly suppressed. As a result, electrons populating the lower laser subband may increase their energy by optical phonon reabsorption what might eventually lead to return of these carriers to the excited states in the upper subband. Such a process should enhance the effective electron lifetime in the latter subband resulting in lowering of the threshold current. This effect was predicted recently<sup>8</sup> for the case of bulklike optical phonons.

The purpose of the present work is to investigate numerically the behavior of the kinetics of the coupled electron-phonon system in a realistic AlGaAs/GaAs QCL active region; this treatment takes into account all essential conditions. This may help in providing valuable insight to the phenomena that eventually determine the performance of the laser. In this context, it is worth mentioning recent interesting experimental measurements in related QC diode and laser structures based on AlGaAs/GaAs heterostructure.<sup>46,47</sup>

In order to verify the theoretical predictions of Ref. 8, our study places strong emphasis on the consideration of the possibility of lowering the lasing threshold currents by means of the reabsorption of confined nonequilibrium optical phonons by quantized electrons.

## II. MODEL

Hot-phonon effects on coupled electron-phonon system relaxation dynamics in an AlGaAs/GaAs quantum cascade laser structure have been investigated numerically by the ensemble Monte Carlo technique. A system of coupled kinetic equations for electrons and phonons, in which both, electron quantization and optical phonon confinement<sup>12</sup> are impor-

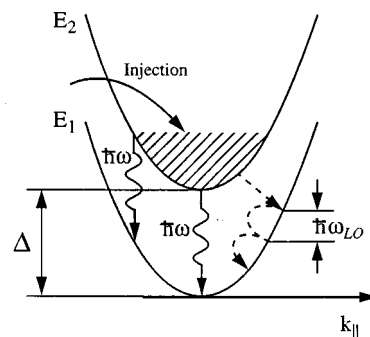


FIG. 1. Simplified schematics of the active quantum-well region of a QCL.

tant, was solved for two different cases: one where hot-optical-phonon buildup is strong and another where such a buildup is negligible. This latter artificial case (usually assumed in theoretical estimations) serves mostly for the illustrative purposes in our study: under realistic device operation conditions, phonon accumulation is significant in the structure. Thus need for the kinetic approach results naturally from the strongly nonequilibrium state of the electron-phonon system in the active region of the QCL.

The simulations were performed for an equilibrium lattice temperature of 10 K which is close to the experimental conditions.<sup>1</sup> We do not consider the whole complex structure of a QC laser in the present work. To study the influence of hot phonons on electron relaxation dynamics in the active GaAs QW region, it is sufficient to consider the following simplified scheme; see Fig. 1. Confinement by AlGaAs/GaAs heterointerfaces forms the quantum well laser system with two lasing subbands separated by a 295 meV energy interval. In reality, these subbands may even belong to several coupled quantum wells; however, our assumption of a single QW is expected to be adequate since horizontal transitions by means of resonant tunneling are fast between these wells and, in most practical cases, do not introduce a significant bottleneck in the electron-phonon phenomena considered.

Electron relaxation in the AlGaAs/GaAs QCL structure consists of several stages. Electrons injected in the active region initially populate the upper energy subband. For simplicity, we assume that carriers are injected with an equilibrium distribution corresponding to the 10-K lattice temperature. In other words, we consider initially a nearly monoenergetic electron flux. This slight deviation from the realistic conditions serves mostly for illustrative purposes.

By means of light emission or phonon-assisted radiationless scattering processes, the carriers transit to the lower laser subband. In this latter case, electrons cool there by the cascade emission of optical phonons what may drive the phonon system substantially out of equilibrium. The emission prevails among phonon-assisted radiationless scattering processes, which also have much larger probabilities than light emission. As mentioned, the presence of the heterointerfaces gives rise to confinement of optical-phonon modes within the active GaAs QW layer.<sup>12</sup> Taking into account that in the material system considered the phonon generation time,  $\tau_g \approx 0.1$  ps, is much less than their decay time,  $\tau_d \approx 8.0$  ps, this

feature is extremely favorable for nonequilibrium phonon accumulation in the structure. It should be also pointed out that the temperature chosen (10 K) is low with respect to the optical-phonon energy for GaAs:  $\hbar\omega_{LO} \approx 36$  meV; therefore, at equilibrium the population of these phonons is very small and their absorption by electrons is thus a scattering mechanism of minor importance. Hence, hot-phonon effects should be well pronounced for such conditions and for the structure parameters chosen.

The energy difference between the bottoms of the two electron subbands supporting the radiative transitions,  $\Delta \approx 295$  meV, is roughly 8.2 times larger than the optical-phonon energy,  $\hbar\omega_{LO}$ , which is  $\approx 36$  meV. As a result, each carrier relaxing in the lower subband may be able to emit successively multiple phonons before thermalizing or escaping from the active QW region, provided that the time of electron removal from this subband,  $\tau_{esc}$ , is larger than the optical phonon emission time,  $\tau_g$ ; it holds true in our model since  $\tau_{esc} \approx 0.5$  ps. This is in contrast to the case of an intersubband carrier transition during which an electron emits just one optical phonon. As we consider later on, optical phonon modes *selectively* participate in electronic transitions, therefore, the discussed differences in phonon mode generation may manifest explicitly during different carrier relaxation stages in the QCL system.

Our simple model accurately takes into account many important features of the band structure and carrier-phonon interaction in the system such as the inelasticity of electron-acoustic-phonon scattering<sup>39</sup> which might be significant at lower temperatures as well as confinement and decay<sup>48</sup> of optical phonon modes.

We use a right-handed orthogonal Cartesian coordinate system for the planar geometry of the QCL structure investigated. The  $x$  and  $y$  axes lie in the GaAs QW plane. The applied electric field,  $E$ , is in the  $z$  direction ( $E_x = E_y = 0$ ); therefore, this field does not have any effect on the in-plane (parallel) electron motion.

In our model, we do not consider electron scattering by remote ionized impurities, regions of surface roughness, and other carriers. Even though these mechanisms may be important at very low temperatures and high electron concentrations,<sup>49,50</sup> they should not play a crucial role in the phenomena investigated herein.

### III. RESULTS AND DISCUSSION

Figure 1 illustrates stationary carrier distributions in the electronic levels for a particular injection current in the case of the *equilibrium* phonon system in the laser structure. As shown in Fig. 1(a), injected electrons reside near the bottom of the upper subband; reminiscent of a Gaussian, the stationary shape of the latter distribution reveals that a quasiequilibrium is established in this carrier subsystem (Fig. 2).

Note that optical-phonon emission dominates in the system even in this case of a near-undisturbed phonons. Largely as a result of this weak interaction, electron heating (smearing of their distribution) in the upper subband is insignificant: carriers preferably lose their energy,  $\epsilon_2$ , by transferring slowly to the lower subband with an intensity,  $R$ :

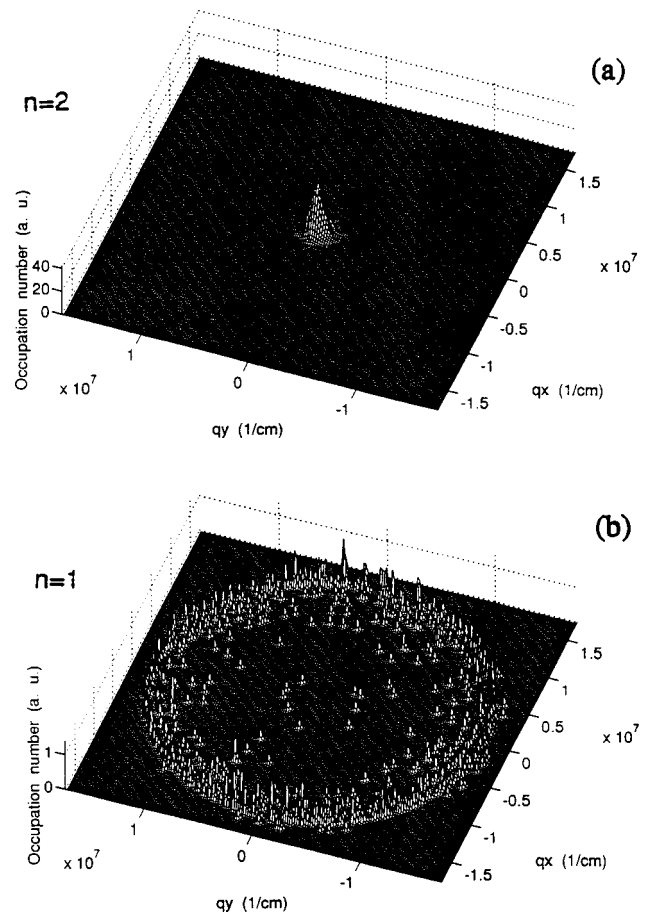


FIG. 2. Electron distributions in the working subbands in the case of undisturbed phonon system; (a) The upper subband, (b) the lower subband. The active GaAs-quantum-well region:  $a = 75.47$  Å,  $j = 30$  kA/cm<sup>2</sup>,  $T = 10$  K.

$$R = A[1 - n_1(\epsilon_2 - \hbar\omega_{LO})](1 + N_q) - A[1 - n_2(\epsilon_2)]N_q, \quad (1)$$

where  $n_2(\epsilon_2)$  and  $n_1(\epsilon_2 - \hbar\omega_{LO})$  are the electron distribution functions of states in the upper and in the lower subbands participating the intersubband transition, respectively;  $N_q$  is the equilibrium phonon occupation number at 10-K lattice temperature, and  $A$  is a constant.

Because  $N_q$  is much less than unity,

$$R' \approx A[1 - n_1(\epsilon_2 - \hbar\omega_{LO})].$$

Evidently, the rate of the intersubband electronic transition is nearly independent of  $N_q$  in the case of equilibrium phonons. This means that dominating the scattering *spontaneous* optical-phonon emission events result in a comparably low intensity for the latter electron transfer process. As a result, significant carrier populations are required in the upper subband to provide an electron flux to the lower laser subband. According to the current continuity law, this carrier flux assures a particular stationary current in the QCL structure, so it can be controlled by varying the external conditions including the injection rate and the lattice temperature.

On the other hand, the absence of a prohibition against the intersubband quasi-two-dimensional (2D) electron scattering accompanied by the prevailing optical-phonon emission, makes the contribution of the radiationless transitions

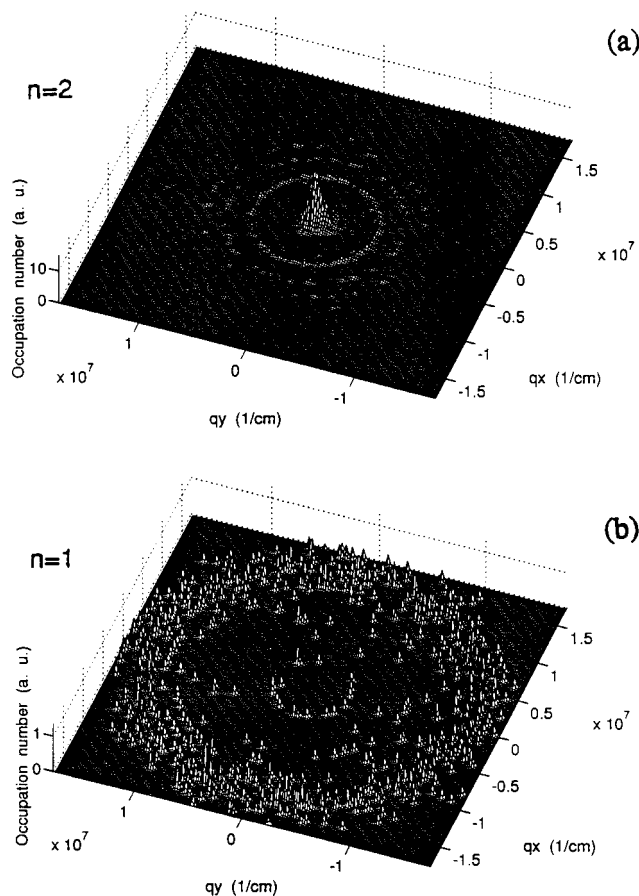


FIG. 3. Electron distributions in the subbands in the case of strong hot-phonon buildup; (a) The upper level, (b) the lower level. The active GaAs-quantum-well region:  $a = 75.47 \text{ \AA}$ ,  $j = 30 \text{ kA/cm}^2$ ,  $T = 10 \text{ K}$ .

quite high compared to that caused by light emission processes. As a result, carrier lifetime in the upper subband is short and large threshold injection currents are therefore required to provide conditions necessary for the required electron population inversion in the active QW region(s).

In contrast to electrons in the upper subband, carriers transferred to the lower subband initially reside at significant energies with respect to this subband bottom; see Fig. 1(b). Here, phonon-mediated carrier energy dissipation processes result in a peaklike accumulation of electron populations at energies equal to multiples of the optical-phonon energy,  $\hbar\omega_{LO}$ . Because the electron distribution in the upper subband is not smeared substantially—as expected for conditions of near monoenergetic injection and *undisturbed* phonons in the system—these carrier population peaks become grouped into a system of concentric “domains” in wave-vector (momentum) space as a result of in-plane isotropy of the structure in the direction perpendicular to  $k_z$  direction (recall that  $E_x = E_y = 0$ ). The distance between these “rings” increases as they converge on the common center coinciding with the subband bottom. This feature follows naturally from the electron and optical phonon energy dispersion relations and the conservation laws for electron-phonon scattering. It can be shown that neighboring carrier population rings are separated equidistantly by the energy-space interval,  $\hbar\omega_{LO}$  (Fig. 3).

For the case of *equilibrium* phonons under consideration, significant electron populations in the lower subband remain concentrated primarily at the high-energy region. In the region near the common center of the ring system, i.e., going in the direction of decreasing energy, carrier populations dramatically diminish. The reason for this is that electrons are rapidly emptied from here as well as from the active region by means of resonant tunneling to a neighboring quantum well. Only a fraction of relaxing carriers in the lower subband eventually reaches the low energy regions; this creates a population inversion with respect to the bottoms of the two laser subbands. It should be pointed out that the subband separation,  $\Delta$ , is chosen not to be a multiple of  $\hbar\omega_{LO}$  in order to prevent electrons from reaching the energy regions close to the lower subband bottom by means of several sequential optical-phonon emission events. This effect helps to create a carrier population inversion in the structure with respect to the bottoms of the lasing electronic subbands. Of course, another necessary condition for the creation of a population inversion is that the rate of the electron escape from the lower subband to a neighboring coupled quantum well must be higher than the rate of carrier injection into the upper level. This carrier injection is, of course, caused by the injection current.

In a realistic case, electrons relaxing in the system generate significant confined nonequilibrium-optical-phonon populations. The energy captured in the structure in the form of hot phonons may be transferred back to electron subsystem causing its additional heating. Even at low lattice temperatures and moderate injection currents, the accumulation of these nonequilibrium phonons may become significant and strongly affect carrier transport parameters in the active GaAs quantum-well region(s). Therefore, in the realistic situation, the physical picture of relaxation phenomena considered is distinctly different from that described previously for the artificial case of equilibrium phonons. Note that for significant hot-optical-phonon populations, *stimulated* phonon emission and reabsorption by electrons become important factors in the coupled electron-phonon system kinetics. As a result, distribution functions of both electrons and phonons, calculated self-consistently, differ substantially from those obtained in the previously discussed case of a near-equilibrium phonon system (Fig. 4).

It should be pointed out that because of the selectivity implied by conservation rules for electron and confined optical-phonon scattering, these nonequilibrium phonon populations keep track of the corresponding electron transitions that were accompanied by these phonon emission. During the decay time of such a phonon mode, an electron may return to its initial state by means of absorption of a corresponding phonon. The latter effect may be especially important in the presence of hot-phonon mode confinement when these phonons become trapped inside the active QW region(s). We have investigated in detail the case of *nonequilibrium optical phonons*, paying much attention to the possibility of lowering the threshold currents by increasing the effective lifetime of the electrons in the upper subband as a result of the reabsorption of these phonons (Fig. 4).

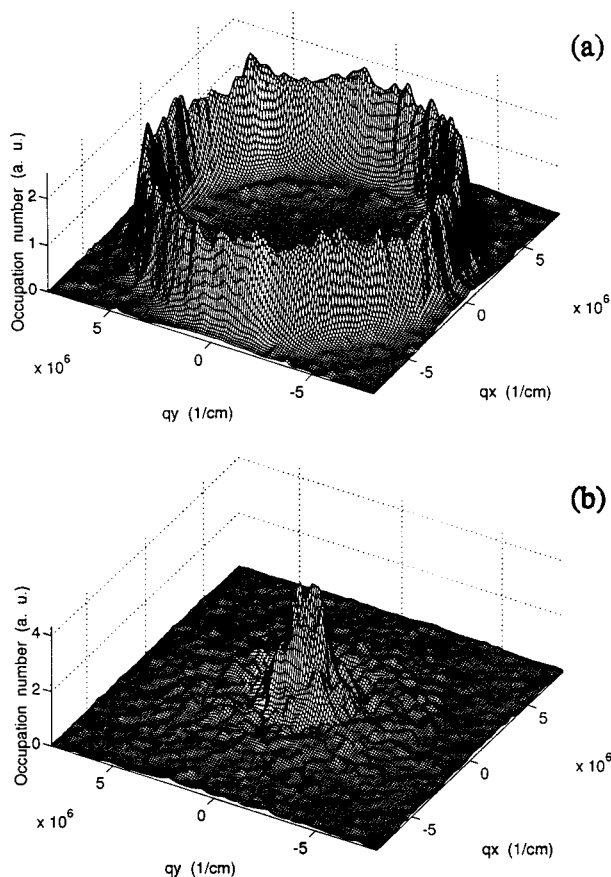


FIG. 4. Hot-optical-phonon distributions in the case of self-consistent approach that takes into account nonequilibrium phonons; (a) the intrasubband phonon mode, (b) the intersubband phonons. The active GaAs-quantum-well region:  $a = 75.47 \text{ \AA}$ ,  $j = 30 \text{ kA/cm}^2$ ,  $T = 10 \text{ K}$ .

Under *hot-phonon* conditions, intrasubband electron relaxation in both working subbands becomes strongly coupled by the means of mutual optical-phonon mode exchange; indeed, it becomes possible for electrons populating a particular subband to interact with phonons emitted not only by the same subband carriers but also with phonons generated by electrons in the other subband. On the other hand, an important issue is that the role of different confined-optical-phonon modes is *different for inter- and intrasubband electron relaxation*. Due to selection rules implied by the energy and momentum conservation for 2D electron and confined optical-phonon systems interaction, certain phonon modes participate *only in intra- or only in intersubband* carrier scattering processes. As a result, the influence of the “intrasubband” and “intersubband” optical phonon modes on electron relaxation can be easily distinguished and considered separately.

As illustrated in Fig. 4(a), electrons reabsorb the intrasubband phonons accumulated primarily by the carriers relaxing in the lower laser subband; hence, the carriers in the upper subband transfer from regions near the subband bottom to the higher-energy regions; compare with Fig. 4(a). In fact, the processes of successive optical-phonon absorption by carriers can be substantially enhanced in this case. These processes result in forming of population peaks (the rings) at energies multiple to the optical-phonon energy; this behavior

is similar to that of the electrons relaxing in the lower laser subband. Note that in this case it is possible for carriers to transfer to the lower subband not only from the upper subband bottom but also from the other populated regions of higher energies. As a result, the diameter of the most outer ring in the lower subband becomes larger, the carrier population does not have such a well-defined border; see Fig. 4(b). These changes of the electron distribution clearly indicate that due to the mutual interaction with the hot phonons confined within the active region, the mean carrier energy (the effective temperature of the electron subsystem) substantially increases. However, the effect does not help to improve the conditions for the population inversion in the active region; indeed, due to the nonparabolicity of electronic subbands only certain energy regions close to the bottoms of the two laser subbands can participate in the radiative transitions accompanied by near monochromatic light emission. In other words, only electron populations in these regions should be taken into account in considering the population inversion. Due to interaction with nonequilibrium optical phonons, heated electrons escape from such regions in the upper subband and cause a reduction of the relative population inversion in the structure. (Note that the described carrier-lattice self-heating effects on carriers relaxing in the lower subband are favorable for improving the population inversion conditions in the active region.)

Strong electron coupling with optical phonons results in parallel changes evident in the nonequilibrium phonon system, as illustrated in Figs. 4(a) and 4(b). These changes are more pronounced for the intrasubband optical phonons [Fig. 4(b)] because their accumulation predominates slightly in the QCL structure under realistic conditions (Fig. 5).

It should be mentioned that probabilities of the previously discussed intra/intersubband electronic transitions, and the generation rate of the corresponding phonon modes, are primarily controlled by the amount of momentum transfer that an electron has to exchange with the lattice during the emission/absorption of optical phonons: the larger the momentum transfer, the lower this probability. Accordingly, from simple geometrical considerations based on Fig. 1, it follows that for the realistic QCL structure investigated, the probabilities of the intrasubband scattering processes are slightly higher than those of the intersubband processes. In fact, the latter may be varied by changing the relative distance between the bottoms of the lasing subbands, i.e., the width of the active QW region(s).

The above consideration does not necessarily mean that the optical phonons created as a result of the intrasubband electronic transition should dominate in the system considered. Basically, the population of the intrasubband phonons can be controlled by changing the effective time of electron removal from the lower subband: the larger this time, the more such phonons accumulated in the active region. In addition, for a given carrier removal time (i.e., the time of resonant tunneling to a neighboring well) this population, naturally, is proportional to the injection current. Note that if the rate of the carrier escape is higher than the phonon generation rate, i.e., if  $\tau_{\text{esc}} < \tau_g$ , the occupation numbers of these phonons will coincide with near-equilibrium ones, indicating

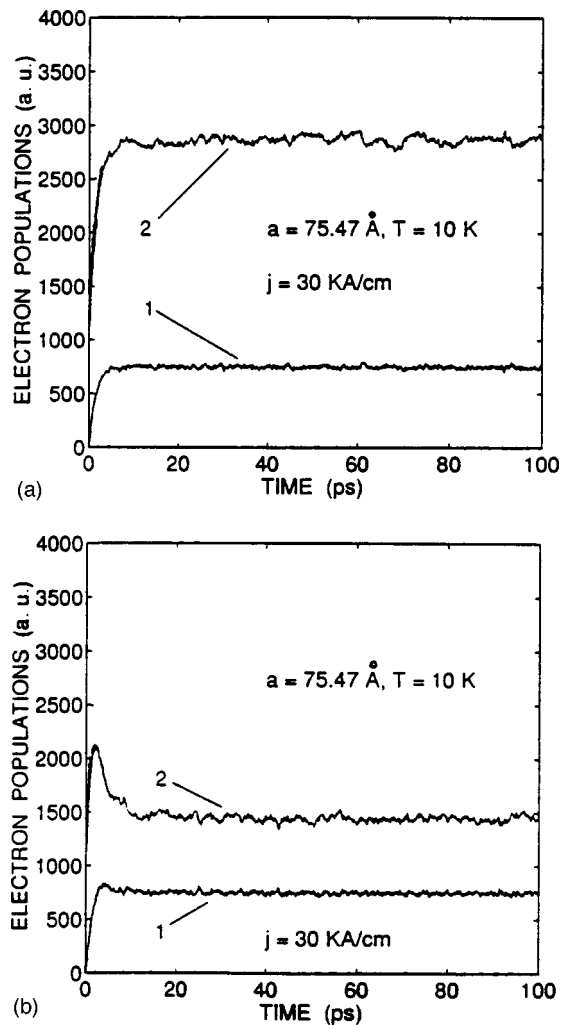


FIG. 5. Temporary evolution of electron populations in the working subbands. The active GaAs-quantum-well region:  $a = 75.47 \text{ \AA}$ ,  $j = 30 \text{ kA/cm}^2$ ,  $T = 10 \text{ K}$ . (a) The case of equilibrium phonon system; (b) the case with hot phonons.

practically undisturbed conditions. According to Fig. 4(b), this is not a case for the QCL structure studied; here there is a washed out system of the intrasubband optical phonon population peaks and the widely spread out momentum space distribution which indicate strongly nonequilibrium conditions and significant energy stored in the phonon subsystem. In some sense, this hot-phonon subsystem serves as a reservoir that takes energy from relaxing electrons in the lower subband and provides additional energy to carriers in the upper subband by means of electron reabsorption of optical phonons. In other words, at steady state the population of the intrasubband phonon modes maintains a certain dynamic energy balance between the coupled electron and phonon subsystems.

As illustrated by Fig. 4(a), the distribution of the intrasubband optical phonons forms a quite complex, symmetrical momentum-space structure in agreement with a complicated dynamics of the overlapping carrier-phonon relaxation processes. On the contrary, for the intersubband electronic transition responsible nonequilibrium optical phonons form a relatively simple smooth single-ring-like structure in mo-

mentum space; see Fig. 1(b). It should be pointed out that the population ring also represents a superposition of the phonons emitted by electrons transiting to the lower level from various populated regions in the upper subband; Fig. 1(a). However, because of the insignificant contribution of the nonparabolicity of the latter subband at energies of several  $\hbar\omega_{LO}$  above the subband bottom, where most of the carriers are concentrated, the conditions for phonon emission are similar. This results in a comparably homogeneous distribution of intersubband optical phonons as depicted in Fig. 4(b).

It is seen in Figs. 4(a) and 4(b) that near the center of momentum space, both intrasubband and intersubband hot-optical-phonon distributions remain undisturbed in accordance with the conservation rules for the electron-optical phonon scattering. On the other hand, the occupation numbers of hot optical phonons become large in certain regions of momentum space.  $N_q \gg 1$  in these regions and Eq. (1) takes on the following form:

$$R' = A[n_2(\epsilon_2) - n_1(\epsilon_2 - \hbar\omega_{LO})]N_q.$$

This expression indicates that the *induced* nonequilibrium-phonon emission and absorption—whose rates increase substantially in comparison with the case of equilibrium phonons—must play a very important role in the structure dynamics.

As discussed previously, at steady state the intersubband electron transition rate is nearly independent on the negligible intersubband phonon mode population in the case of an *undisturbed* phonon system: dominating *spontaneous* optical phonon emission results in a low intensity of the latter carrier transfer process. For the case of *hot-phonons*, the above conditions do not hold any longer due to dramatically increased *induced* optical-phonon emission and absorption.

The induced intersubband optical-phonon reabsorption, whose rate approaches the rate of emission of the corresponding phonon mode, causes a substantial return of electrons to the higher lasing subband, favorable for increasing carrier lifetime there. However, as the above equation indicates, the intersubband electron transition rate is linearly proportional to the intersubband optical-phonon mode population in the case of strong hot-phonon feedback. This means that the induced phonon emission overrides the absorption anyway and remains the governing factor in the structure kinetics.

Because of the dramatically enhanced intersubband optical phonon emission as well as the rate of electron transitions to the lower level, a smaller number of carriers is required in the upper subband in order to provide a stationary carrier flux to the lower subband which is responsible for assuring a particular steady state current in the structure. This factor dominates in intersubband electron relaxation and results in a decrease of the effective carrier lifetime in the upper subband and in a corresponding increase of the threshold current.

The latter effect is illustrated in Fig. 5 where the temporary evolution of electron populations in the lasing subbands is depicted in the case of equilibrium phonons (a) and for the case of the pronounced hot-phonon buildup (b). It is seen

that at steady state the absolute (integral) carrier population inversion is achieved between the two subbands in the case of undisturbed phonons; see Fig. 5(a). On the other hand, Fig. 5(b) indicates that for the same injection current the nonequilibrium-phonon buildup results in significant reduction of the population inversion. In addition, heating of electrons accompanied with spreading of their distribution causes significant electron escape from the radiative-active energy regions near the upper subband bottom and this has also a negative influence on achieving conditions for lasing.

As shown, the feedback of *confined nonequilibrium* optical phonons in the active QW region(s) of the QCL eventually cause substantial increase in the threshold current. Even in the case of bulklike phonon modes, the effect remains qualitatively the same (but, naturally, weaker) because there still exists a certain selectivity imposed by the conservation laws for intra- and intersubband electron scattering: optical phonons with *distinctly different* wave vectors mediate these carrier relaxation processes. The phonon mode generation is also affected by different factors. This finally causes a physical situation for bulklike phonons not much different qualitatively from that one we have investigated in the present article.

#### IV. SUMMARY

Using the Monte Carlo technique, we have investigated hot-optical-phonon effects on coupled electron-phonon system relaxation in an AlGaAs/GaAs quantum cascade laser structure at 10–K temperature.

Our simulation results demonstrate that a strong buildup of confined nonequilibrium optical phonons results in a substantial decrease of carrier intrasubband cooling rates and in strong coupling of electron relaxation in both laser subbands by means of phonon-induced mutual exchange. As a result of hot-phonon accumulation in the structure, electron and phonon distributions are smeared out substantially with a corresponding increase in their characteristic temperatures. The latter effect is not favorable for enhancing the electron population inversion because the nonparabolicity of the subbands restricts the range of energies from which lasing can take place.

We have considered in detail the possibility of increasing the effective lifetime of carriers in the upper lasing subband—and the consequent lowering of the lasing threshold currents—as a result of carrier return there from the lower level by means of induced hot-optical-phonon reabsorption. Unfortunately, the simulation results reveal that under realistic conditions the complete role of hot phonons is the opposite; indeed, they cause substantial electron heating in the subbands and significant induced optical-phonon emission. Both of these phenomena reduce the electron population inversion and lead to the need to further increase the threshold currents.

#### ACKNOWLEDGMENTS

The authors would like to express their gratitude to Dmitri Romanov and Boris Glavin for helpful discussions and critical remarks. This work was supported by the U. S. Army Research Office.

- <sup>1</sup>J. Faist, F. Capasso, D. L. Sivko, C. Sirtori, A. L. Hutchinson, and A. Y. Cho, *Science* **264**, 553 (1994).
- <sup>2</sup>C. Sirtori, J. Faist, F. Capasso, D. L. Sivko, A. L. Hutchinson, and A. Y. Cho, *Superlattices Microstruct.* **19**, 357 (1996).
- <sup>3</sup>J. Faist, F. Capasso, C. Sirtori, D. L. Sivko, A. L. Hutchinson, S. N. G. Chu, and A. Cho, *Superlattices Microstruct.* **19**, 337 (1996).
- <sup>4</sup>J. Faist, F. Capasso, D. L. Sivko, A. L. Hutchinson, C. Sirtori, S. N. G. Chu, and A. Y. Cho, *Appl. Phys. Lett.* **65**, 2901 (1994).
- <sup>5</sup>J. Faist, F. Capasso, C. Sirtori, D. L. Sivko, A. L. Hutchinson, and A. Y. Cho, *Appl. Phys. Lett.* **66**, 538 (1995).
- <sup>6</sup>J. Faist, F. Capasso, C. Sirtori, D. L. Sivko, A. L. Hutchinson, M. S. Hybertsen, and A. Y. Cho, *Phys. Rev. Lett.* **76**, 411 (1996).
- <sup>7</sup>J. Faist, F. Capasso, C. Sirtori, D. L. Sivko, A. L. Hutchinson, and A. Y. Cho, *Electron. Lett.* **32**, 560 (1996).
- <sup>8</sup>V. F. Elesin and Yu. V. Kopaev, *Solid State Commun.* **96**, 897 (1995).
- <sup>9</sup>V. F. Elesin and Yu. V. Kopaev, *JETP* **81**, 1192 (1995).
- <sup>10</sup>M. V. Kisin, V. B. Gorfinkel, M. A. Strosio, G. Belenky, and S. Luryi, *J. Appl. Phys.* **82**, 2031 (1997).
- <sup>11</sup>M. A. Strosio, *J. Appl. Phys.* **80**, 6864 (1996).
- <sup>12</sup>N. Mori and T. Ando, *Phys. Rev. B* **40**, 6175 (1989).
- <sup>13</sup>P. J. Price, *Physica B* **134**, 164 (1985).
- <sup>14</sup>M. Rieger, P. Kocevar, P. Lugli, P. Bordone, L. Regianni, and S. M. Goodnick, *Phys. Rev. B* **39**, 7866 (1989).
- <sup>15</sup>W. Cai, M. C. Marchetti, and M. Lax, *Phys. Rev. B* **37**, 2636 (1988).
- <sup>16</sup>J. Shah, R. C. C. Leite, and J. F. Scott, *Solid State Commun.* **8**, 1089 (1970).
- <sup>17</sup>D. Y. Oberli, G. Böhm, and G. Weimann, *Phys. Rev. B* **47**, 7630 (1993).
- <sup>18</sup>K. T. Tsen, R. P. Joshi, D. K. Ferry, A. Botchkarev, B. Sverdlov, A. Salvador, and H. Morkoc, *Appl. Phys. Lett.* **68**, 2990 (1996).
- <sup>19</sup>E. D. Grann, K. T. Tsen, and D. K. Ferry, *Phys. Rev. B* **53**, 9847 (1996).
- <sup>20</sup>P. Kocevar, *Physica B* **134**, 155 (1985).
- <sup>21</sup>T. Ruf, K. Wald, P. Yu, K. Tsen, H. Morcoč, and K. Chan, *Superlattices Microstruct.* **13**, 203 (1993).
- <sup>22</sup>R. Mickevičius and A. Reklaitis, *J. Phys.: Condens. Matter* **2**, 7883 (1990).
- <sup>23</sup>K. Leo, W. Rühle, and K. Ploog, *Solid-State Electron.* **32**, 1863 (1989).
- <sup>24</sup>P. Blockmann, J. Young, P. Hawrylak, and H. M. van Driel, *Semicond. Sci. Technol.* **9**, 746 (1994).
- <sup>25</sup>K. Santra and C. Sarkar, *Phys. Rev. B* **47**, 3598 (1993).
- <sup>26</sup>F. Vallee and F. Bogani, *Phys. Rev. B* **43**, 12 049 (1991).
- <sup>27</sup>K. Kim, K. Hess, and F. Capasso, *Appl. Phys. Lett.* **52**, 1167 (1988).
- <sup>28</sup>P. Lugli and D. K. Ferry, *IEEE Trans. Electron Devices* **32**, 2431 (1985).
- <sup>29</sup>S. M. Goodnick and P. Lugli, *Phys. Rev. B* **37**, 2578 (1988).
- <sup>30</sup>R. Mickevičius and A. Reklaitis, *Solid State Commun.* **64**, 1305 (1987).
- <sup>31</sup>S. Koch and T. Mizutani, *IEEE Trans. Electron Devices* **41**, 1498 (1994).
- <sup>32</sup>K. Kurishima, H. Nakajima, T. Kobayashi, Y. Matsuoka, and T. Ishibashi, *IEEE Trans. Electron Devices* **41**, 1319 (1994).
- <sup>33</sup>R. Kubur, J. Schmid, and R. Popovich, *IEEE Trans. Electron Devices* **41**, 315 (1994).
- <sup>34</sup>N. S. Mansour, Y. M. Sirenko, K. W. Kim, M. A. Littlejohn, J. Wang, and J. P. Leburton, *Appl. Phys. Lett.* **67**, 3480 (1995).
- <sup>35</sup>G. Fasol, M. Tanaka, H. Sakaki, and Y. Horikosh, *Phys. Rev. B* **38**, 6056 (1988).
- <sup>36</sup>P. Hawker, A. Kent, O. Hughes, and L. Challis, *Semicond. Sci. Technol.* **7**, 29 (1992).
- <sup>37</sup>K. W. Kim, M. A. Strosio, A. Bhatt, R. Mickevičius, and V. V. Mitin, *J. Appl. Phys.* **70**, 319 (1991).
- <sup>38</sup>R. Mickevičius, V. V. Mitin, K. W. Kim, M. A. Strosio, and G. J. Iafrate, *J. Phys.: Condens. Matter* **4**, 4959 (1992).
- <sup>39</sup>R. Mickevičius, V. Mitin, U. K. Harithsa, D. Jovanovic, and J. P. Leburton, *J. Appl. Phys.* **75**, 973 (1994).
- <sup>40</sup>W. Shockley, *Bell Syst. Tech. J.* **30**, 990 (1951).
- <sup>41</sup>S. Komiyama, *Adv. Phys.* **31**, 255 (1982).

- <sup>42</sup>D. Jovanovic and J. P. Leburton, *Superlattices Microstruct.* **11**, 141 (1992).
- <sup>43</sup>V. V. Mitin, G. Paulavičius, N. Bannov, and M. A. Strosio, *J. Appl. Phys.* **79**, 8955 (1996).
- <sup>44</sup>V. V. Mitin, G. Paulavičius, and N. A. Bannov, *Superlattices Microstruct.* (to be published).
- <sup>45</sup>R. Mickevičius, V. Mitin, G. Paulavičius, V. Kochelap, M. A. Strosio, and G. J. Iafrate, *J. Appl. Phys.* **80**, 5145 (1996).
- <sup>46</sup>G. Strasser, P. Kruck, M. Helm, J. N. Heyman, and E. Gornik, *Appl. Phys. Lett.* **71**, 2892 (1997).
- <sup>47</sup>O. Gauthier-Lafaye, P. Boucaud, F. H. Julien, S. Sauvage, S. Cabaret, V. Thierry-Mieg, and R. Planel, *Appl. Phys. Lett.* **71**, 3619 (1997).
- <sup>48</sup>K. Kral, *Phys. Status Solidi B* **174**, 209 (1992).
- <sup>49</sup>J. P. G. Taylor, K. J. Hugill, D. D. Vvedensky, and A. MacKinnon, *Phys. Rev. Lett.* **67**, 2359 (1991).
- <sup>50</sup>J. A. Nixon and J. H. Davies, *Phys. Rev. B* **41**, 7929 (1990).